Electronic Supplementary Information

$MAPbI_{3-x}Br_x$ mixed halide perovskite for fully printable mesoscopic solar cells with enhanced efficiency and less hysteresis

Kun Cao, Hao Li, Shuangshuang Liu, Jin Cui, Yan Shen and Mingkui Wang*

Michael Grätzel Center for Mesoscopic Solar Cells, Wuhan National Laboratory for Optoelectronics, Huazhong University of Science and Technology, 1037 Luoyu Road, 430074 Wuhan, P. R. China. E-mail: mingkui.wang@mail.hust.edu.cn

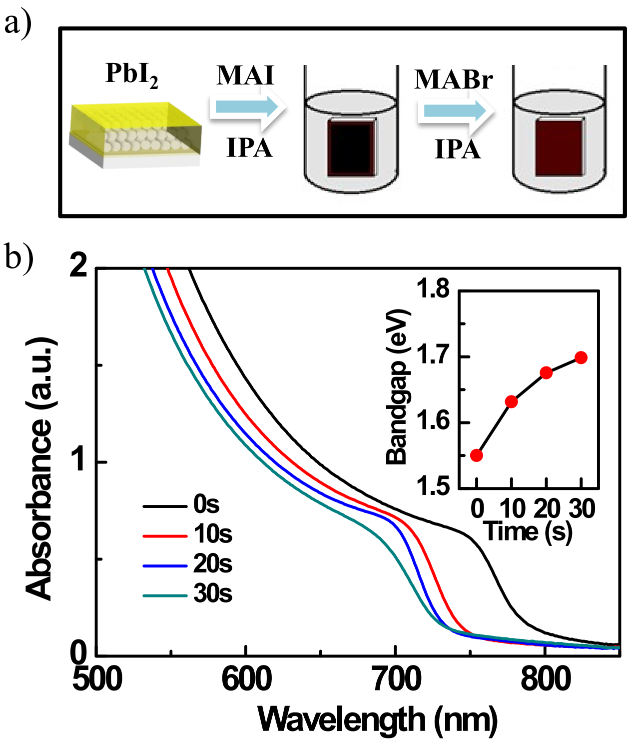

Figure S1 a)Schematic procedures for preparation of the parent $MAPbI_3$ film by the two-step method and transformation to $MAPbI_{3-x}Br_x$ film via halide exchange process. b) UV-vis absorption spectra of the parent $MAPbI_3$ film and $MAPbI_{3-x}Br_x$ films obtained with the different time from 10 s to 30s. The inset gives the plot of the band-gaps of the samples versus dipping time in the MABr/IPA solution (5mg mL^{-1}).

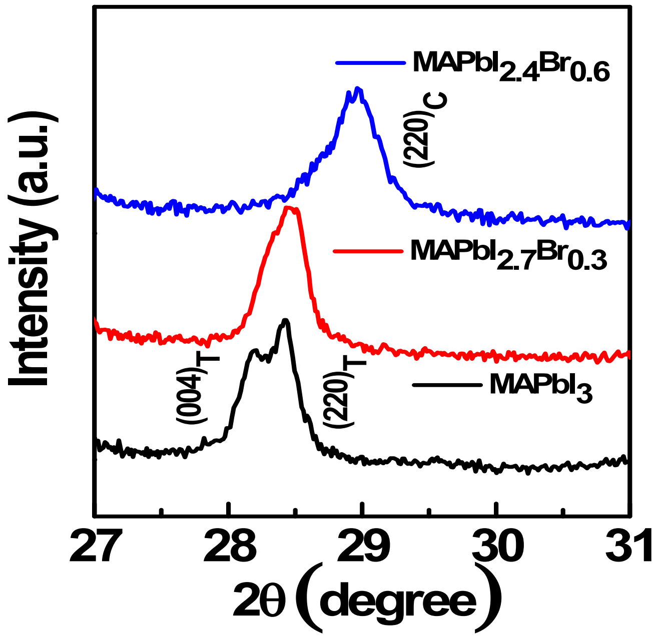

Figure S2 XRD patterns of the $MAPbI_{2.7}Br_{0.3}$ film, $MAPbI_{2.4}Br_{0.6}$ and $MAPbI_3$ film magnified in the region of the tetragonal $(004)_T$ and $(220)_T$ and cubic $(200)_C$ peaks (2θ =27-30°).

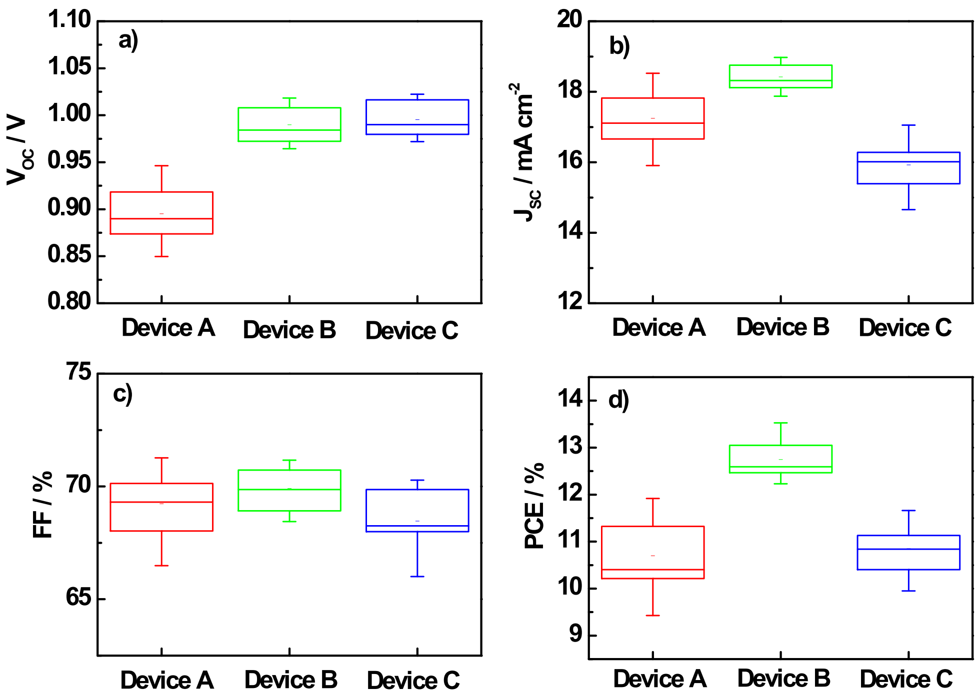

Figure S3 Statistical V_{OC} (a), J_{SC} (b), FF (c) and PCE (d) of 10 devices of device A $TiO_2/Al_2O_3/C(MAPbI_3)$, device B $TiO_2/Al_2O_3/C(MAPbI_{2.7}Br_{0.3})$, and device C $TiO_2/Al_2O_3/C(MAPbI_{2.4}Br_{0.6}$,respectively.

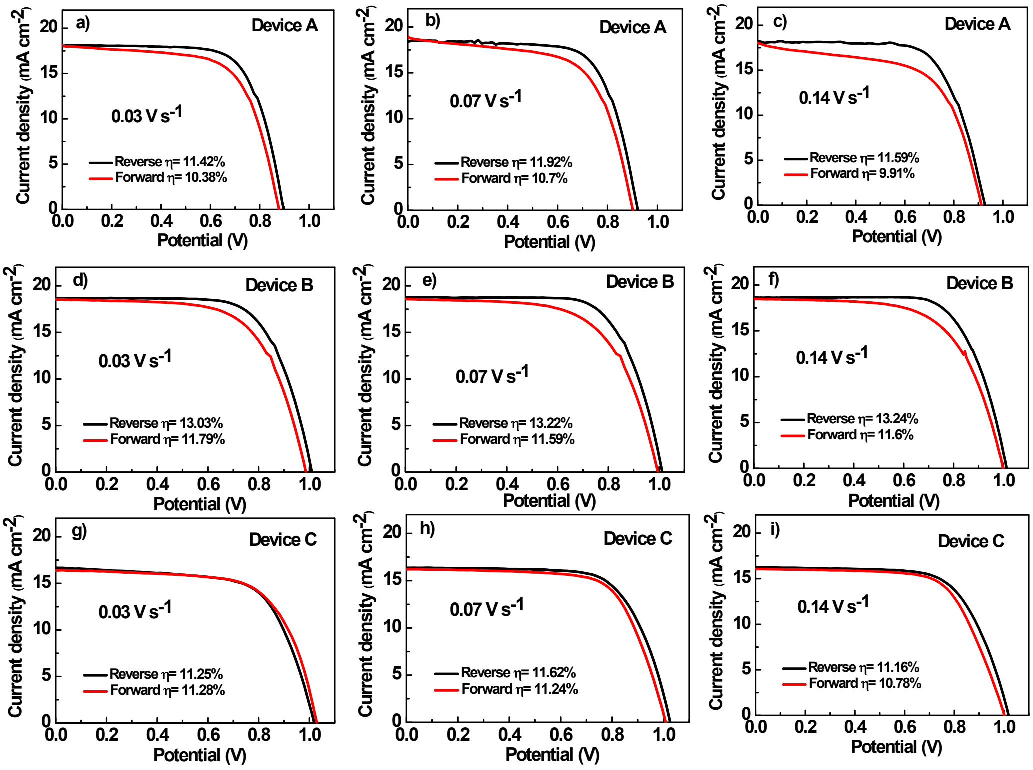

Figure S4 Influence of scanning conditions on J-V curves of device A (a) 0.03 V s^{-1}; b) 0.07 V s^{-1}; and c) 0.14 V s^{-1}), device B (d) 0.03 V s^{-1}; e) 0.07 V s^{-1}; and f) 0.14 V s^{-1})and device C (g) 0.03 V s^{-1}; h) 0.07 V s^{-1}; and i) 0.14 V s^{-1}). From forward bias to short circuit (reverse) and from short circuit to forward bias (forward) cell measured under simulated AM1.5 100 mW cm^{-2} sun.

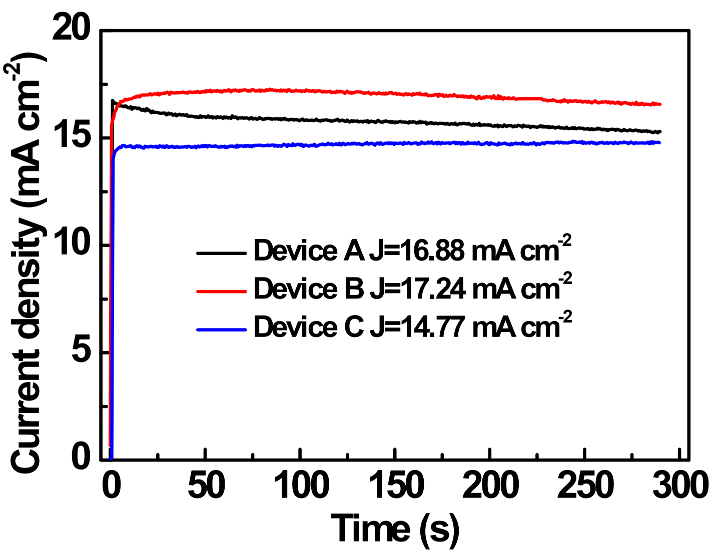

Figure S5 Photocurrent density as a function of time for the device A $TiO_2/Al_2O_3/C(MAPbI_3)$, device B $TiO_2/Al_2O_3/C(MAPbI_{2.7}Br_{0.3})$, and device C $TiO_2/Al_2O_3/C(MAPbI_{2.4}Br_{0.6}$, held at a forward bias of maximum output power point (0.71 V for device A, 0.76V for device B, and 0.77V for device C). The cell was placed in the dark prior to the start of the measurement.

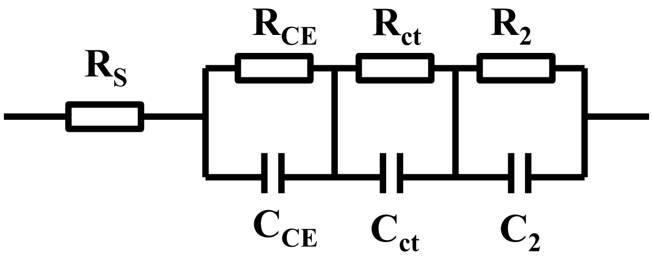

Figure S6 The equivalent circuit for fitting of electronic impedance spectroscopy under illumination.

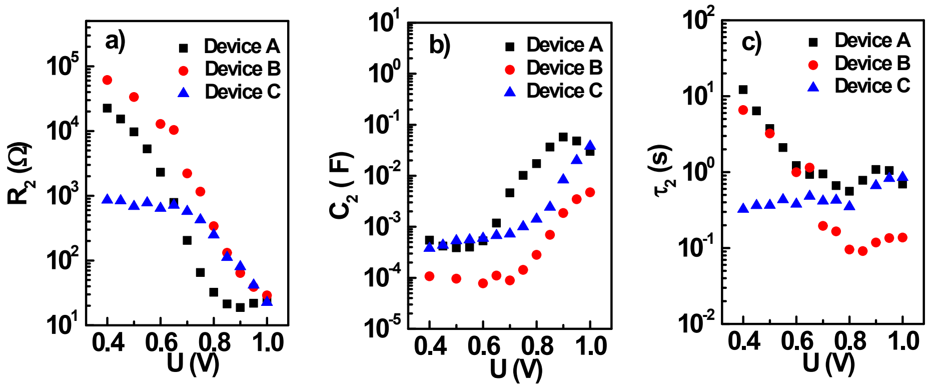

Figure S7 Derived equivalent circuit components obtained from impedance measurements under light for three different devices: a) the low frequency resistance R_2; b) the corresponding capacitance C_2; and c) the calculated time constant τ_2 for devices A $TiO_2/Al_2O_3/C(MAPbI_3)$ (black), device B $TiO_2/Al_2O_3/C(MAPbI_{2.7}Br_{0.3})$ (red), and device C $TiO_2/Al_2O_3/C(MAPbI_{2.4}Br_{0.6})$ (blue).

Figure S7 shows the obtained low frequency resistance R_2 as a function of bias. Interestingly, the larger R_2 results are displayed for the device B and C based on $MAPbI_{3-x}Br_x$ at a given bias over about 0.70 V compared with that of device A with $MAPbI_3$. It needs to note that the R_2 results are comparable to the R_{ct} results in $TiO_2/MAPbI_3$ interface at this given bias region. The relation between the R_2 and the applied potential in this region shows similar characteristics with that of R_{ct} in $TiO_2/MAPbI_3$ interface. Therefore, we assume that in the high bias the resistance R_2 at low frequency shows the characteristics of interfacial recombination resistance, providing an indication of the interfacial recombination resistance. Similarly, the capacitance C_2-voltage character also shows charge accumulation features in the region of exceeding 0.6-0.95 V being almost 2 orders of magnitude larger than the electron accumulation capacitance C in the middle frequency region. Figure S7c presents the calculated time constant τ_2 for the slow dielectric response of the perovskite material. It was observed that the τ_2 of the devices based on $MAPbI_{3-x}Br_x$ perovskite were much lower than that of $MAPbI_3$-based device. For device C, the τ_2 shows small change when the applied bias deceased. The slow dielectric response of the perovskite material, which is given by the low frequency feature of EIS, has been cited as a possible source of the anomalous hysteresis seen in perovskite solar cells.

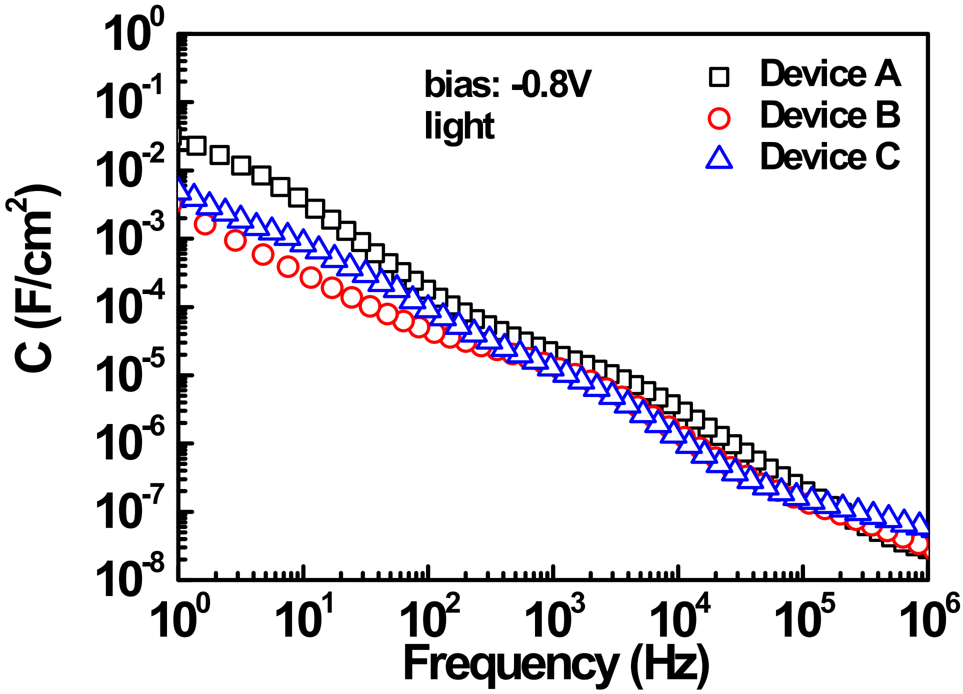

Figure S8 Frequency-dependent capacitance obtained from impedance measurements under light for three different devices: a) the low frequency resistance R_2; b) the corresponding capacitance C_2; and c) the calculated time constant τ_2 for devices A $TiO_2/Al_2O_3/C(MAPbI_3)$ (black), device B $TiO_2/Al_2O_3/C(MAPbI_{2.7}Br_{0.3})$ (red), and device C $TiO_2/Al_2O_3/C(MAPbI_{2.4}Br_{0.6})$ (blue).